## Mechanism of a Dually Catalyzed Enantioselective Oxa-Pictet-Spengler Reaction and the Development of a Stereodivergent Variant

Alafate Adili,¹ John-Paul Webster,² Chenfei Zhao,³ Sharath Chandra Mallojjala,² Moises A. RomeroReyes,¹ Ion Ghiviriga,⁴ Khalil A. Abboud,⁵ Mathew J. Vetticatt,\*,² and Daniel Seidel¹,\*

- <sup>1</sup> Center for Heterocyclic Compounds, Department of Chemistry, University of Florida, Gainesville, Florida 32611, United States
- <sup>2</sup> Department of Chemistry, Binghamton University, Binghamton, New York 13902, United States.
- <sup>3</sup> Department of Chemistry and Chemical Biology, Rutgers, The State University of New Jersey, Piscataway, New Jersey o8854, United States
- <sup>4</sup> Center for NMR Spectroscopy, Department of Chemistry, University of Florida, Gainesville, Florida 32611, United States.
- <sup>5</sup> Center for X-ray Crystallography, Department of Chemistry, University of Florida, Gainesville, Florida 32611, United States.

Supporting Information Placeholder

**ABSTRACT:** Enantioselective oxa-Pictet–Spengler reactions of tryptophol with aldehydes proceed under weakly acidic conditions utilizing a combination of two catalysts, an indoline HCl salt and a bisthiourea compound. Mechanistic investigations revealed the roles of both catalysts and confirmed the involvement of oxocarbenium ion intermediates, ruling out alternative scenarios. A stereochemical model was derived from DFT calculations, which provided the basis for the development of a highly enantioselective stereodivergent variant with racemic tryptophol derivatives.

**Keywords**: oxa-Pictet–Spengler reaction, asymmetric catalysis, dual catalysis, anion-binding catalysis, oxocarbenium ions, kinetic isotope effects, DFT calculations

Oxa-Pictet-Spengler reactions represent an attractive method for accessing various cyclic ethers including isochromans and tetrahydropyrano[3,4-b]indoles, compounds of significant interest in synthetic and medicinal chemistry.1 Although the first oxa-Pictet-Spengler reaction was published already in 1935,2 progress in developing catalytic enantioselective variants has been slow and remains limited to relatively few examples.3 In contrast, many variants of catalytic enantioselective Pictet-Spengler reactions have been developed.<sup>4</sup> This disparity reflects the difficulty in controlling enantioselectivity in reactions involving oxocarbenium ions, in particular when these reactive intermediates are generated via the direct condensation of an alcohol with an aldehyde. In fact, the vast majority of catalytic enantioselective reactions reported to date which involve oxocarbenium ions generate these intermediates from acetals and enol ethers.<sup>5,6</sup> The first publications on highly enantioselective oxa-Pictet-Spengler reactions did not appear until 2016. At that time, some of us reported enantioselective oxa-Pictet-Spengler reactions of tryptophol with aldehydes, utilizing a combination of chiral bisthiourea catalyst 1a and (S)-indoline-2-carboxylic acid methyl ester hydrochloride (2a°HCl) (Scheme 1a).3d Simultaneously, the List group disclosed related reactions with β-phenylethanols and aldehydes, employing a highly

acidic imidodiphosphoric acid (IDP) catalyst (Scheme 1b).<sup>3e</sup> Scheidt and coworkers later reported catalytic enantioselective oxa-Pictet–

#### Scheme 1. Catalytic enantioselective oxa-Pictet-Spengler reactions.

Spengler cyclizations of tryptophol derivatives containing an enol ether moiety.<sup>3f, 3h</sup> Their cooperative catalysis approach is based on a chiral phosphoric acid catalyst and an achiral urea cocatalyst (Scheme 1c). More recently, our group reported Brønsted acid catalyzed enantioselective oxa-Pictet–Spengler reactions of

PhMe, 5 Å MS, -30 °C, 24 h

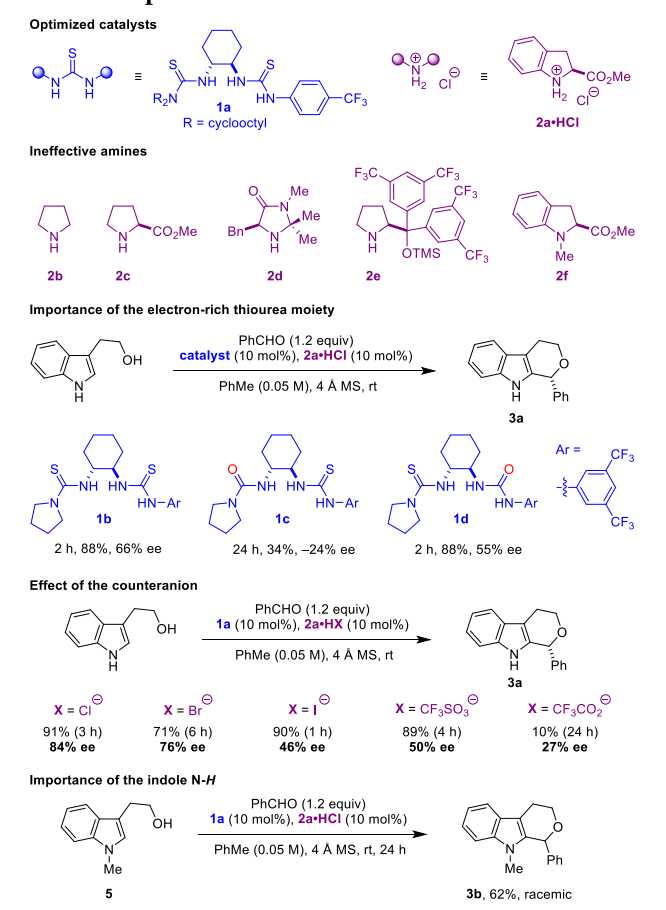
Figure 1. Plausible mechanistic scenarios.

tryptophol and ketals, providing dihydropyran products containing a tetrasubstituted stereogenic center (Scheme 1d).<sup>3g</sup> Of these approaches, our original dual catalysis method (Scheme 1a) stands out as it operates under relatively weakly acidic conditions. Here we report a mechanistic analysis of this process, along with a stereochemical model. In addition, we present a stereodivergent variant with racemic tryptophol derivatives, the development of which was informed by insights gained from our computational studies.

The originally envisioned catalytic cycle for our dual catalysis approach7 to the oxa-Pictet Spengler reaction is outlined in Figure 1a. When used in equimolar amounts, catalysts 1a and 2a•HCl, at least to some extent, likely exist as the ion pair I. Addition of an aldehyde to the catalyst mixture enables the formation of iminium ion pair II with concomitant loss of water. Nucleophilic 1,2-attack of the iminium ion by the hydroxyl group of tryptophol then generates protonated N,Oacetal ion pair III. Subsequent proton transfer (presumably stepwise) leads to the formation of ion pair IV. This is followed by the elimination of the neutral amine catalyst. furnishing the key oxocarbenium ion pair V. The latter undergoes cyclization followed by deprotonative rearomatization to provide the final product while regenerating ion pair I. An alternative mechanism is provided in Figure 1b. Here, iminium ion pair II is formed in identical fashion but then engages tryptophol via C-C bond formation involving the 2-position of the indole ring. Resulting ion pair VI undergoes proton transfer to form ion pair VII which then suffers loss of the neutral amine catalyst to form azafulvenium ion pair VIII. Subsequent cyclization and then deprotonation generates the final product and ion pair I. In either mechanistic scenario, the amine catalyst<sup>8,9</sup> fulfills the same roles. First, the amine acts as a nucleophile in the generation of iminium ion II, the electrophilicity of which is strongly dependent on the structure of the amine. Following 1,2-attack of II by tryptophol and subsequent proton transfer, the amine catalyst then acts as a leaving group. Notably, there are relatively few examples of asymmetric iminium catalysis in which catalyst turnover is achieved by elimination of the amine.10 While the amine HCl salt is critically important, our data indicate that the enantiodetermining step is controlled exclusively by the bisthiourea catalyst,3d which primarily

functions as a chiral anion receptor.<sup>11,12</sup> In addition, binding of the bisthiourea catalyst to the chloride anion likely enhances the electrophilicity of the iminium ion in ion pair II relative to the unbound iminium chloride,<sup>13</sup> and increases the leaving group aptitude of the amine in ion pair III or VII. Based on our studies discussed below, the bisthiourea-chloride complex engages in critical interactions with the cationic condensation product derived from tryptophol and the aldehyde (oxocarbenium ion in V or azafulvenium ion in VIII).

# Scheme 2. Structure-activity/selectivity relationships.



In the initial development of the title reaction, we found that (S)-indoline-2-carboxylic acid methyl ester hydrochloride (2a°HCl) is a uniquely effective cocatalyst (Scheme 2).3d No reaction was observed with pyrrolidine hydrochloride (2b•HCl), (S)-proline methyl ester hydrochloride (2c•HCl), or widely used catalysts 2d•HCl<sup>8d</sup> and 2e•HCl.<sup>14</sup> While iminium ions derived from catalysts 2b-e likely lack sufficient electrophilicity to engage tryptophol, the lack of reactivity of the latter two catalysts may further be due to the fact that they were specifically designed to minimize 1,2-addition. Interestingly, (±)-2a•HCl performs nearly identically to the enantiopure catalyst, suggesting that the amine catalyst is not involved in the enantiodetermining step of the reaction. While maintaining the same level of enantioselectivity observed with 2a. HCl, an extremely sluggish reaction was observed with 2f. HCl. Since this amine is incapable of forming iminium ions, this observation seemingly rules out the possibility of the amine salt simply acting as a buffered source of HCl. The importance of an electron-rich thiourea moiety in the anion-binding catalyst becomes apparent when comparing the performance of catalysts **1b** and **1c**. While bisthiourea 1b (an early variant of 1a) performs reasonably well in the oxa-Pictet-Spengler reaction, the corresponding urea-thiourea 1c exhibits a dramatically reduced activity (low conversion after 24 h vs. full conversion in 2 h). In addition, the opposite enantiomer of 3a is obtained in low ee. In contrast, thiourea-urea **1d** is equally active as bisthiourea **1b**, only leading to a slight drop in product ee. These findings suggest that the sulfur atom of the electron-rich thiourea is involved in an important interaction with the substrate in the enantiodetermining step of the reaction. The effect of the counteranion was also evaluated, firmly establishing the role of 1a as an anion receptor (Scheme 2). While other halides and triflate all provided active catalyst systems, chloride furnished the highest ee, with iodide exhibiting the fastest reaction rate. A low level of reactivity was observed with trifluoroacetate. Finally, N-methyl tryptophol (5) reacted sluggishly, even though N-methyl indole is a more potent nucleophile than indole itself. Furthermore, product 3b was obtained in racemic form. These findings illustrate the importance of a free indole N-H moiety which is almost certainly involved in critical interactions enantiodetermining step of the reaction.15

Scheme 3. Studies probing the intermediacy of oxocarbenium and azafulvenium ions.

As outlined in Scheme 3, we conducted several experiments to probe the potential involvement of oxocarbenium and azafulvenium ions. Mixed acetal 4, when exposed to catalytic amounts of HCl and bisthiourea 1a, provided product 3a in a fast reaction. Under otherwise identical conditions, 3a was obtained in a significantly slower reaction when 4 was replaced by a mixture of tryptophol and benzaldehyde dimethyl acetal. Interestingly, conducting the reaction of tryptophol and benzaldehyde dimethyl acetal in the presence of 5 Å molecular sieves instead of 4 Å molecular sieves led to a dramatic increase in the rate of the reaction, presumably due to an improved capture of the methanol byproduct.<sup>16</sup> While not entirely eliminating the possibility of an azafulvenium pathway, taken in concert, these results provide strong support for the involvement of an oxocarbenium ion pair akin to **V** (Figure 1). Strong evidence against the involvement of an azafulvenium intermediate (i.e., ion pair VIII in Figure 1) was obtained by exposing 6 to the reaction conditions. While 6 converted to product 3a in a rather fast reaction, the latter was isolated in nearly racemic form.

Table 1. Optimization of the stereodivergent variant.

en- try	catalyst	time [h]	yield (%)	dra	ee (%)
1	ıb	3	95	1.5:1	59/74
2	1 <b>e</b>	3	95	1.5:1	63/80
3	ıf	2.5	95	1.5:1	62/81
4	ıg	2.5	95	1.5:1	58/79
5	1a	3	90	1.2:1	73/76
6	ıh	3	90	1.2:1	77/83
$7^{\rm b}$	1 <b>a</b>	48	8o	1:1	93/93
$8^{b}$	ıh	48	70	1;1	93/93

<sup>a</sup> The first number corresponds to the *trans*-diastereomer. <sup>b</sup> Reaction was run at 0.05 M concentration at −30 °C.

Based on our development of the asymmetric oxa-Pictet-Spengler reaction with achiral tryptophols and informed by our computational model for stereoinduction (vide infra), we sought to develop a stereodivergent variant of this reaction. Inspection of enantioselectivity-determining transition state  $TS_{CC-R}$  for the asymmetric oxa-Pictet-Spengler reaction reveals that the methylene group that is directly attached to

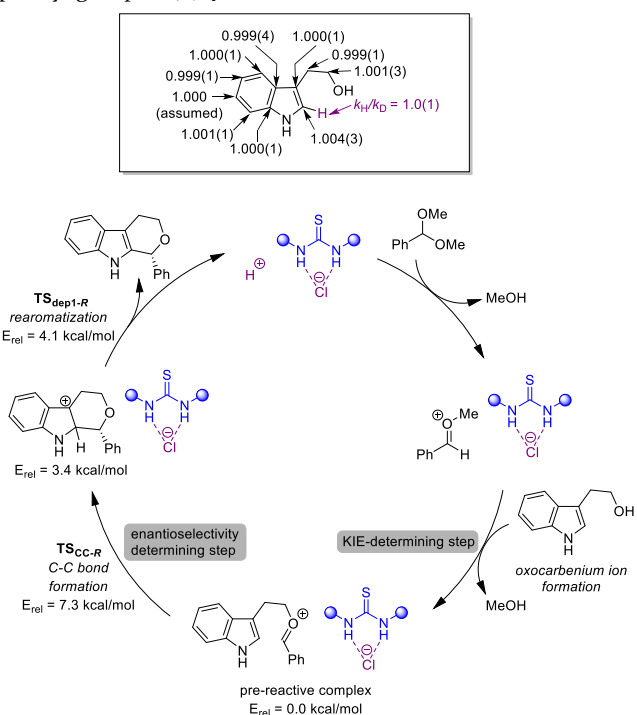
the indole ring is sufficiently far removed from the catalyst to allow for the introduction of a substituent, regardless of the configuration (Figure 2). Either enantiomer of a tryptophol such as **7a** should perform equally well, with the catalyst retaining control over the

Scheme 4. Scope of the stereodivergent reaction.

newly formed stereogenic center. In essence, this would amount to a stereodivergent process in which each enantiomer of the racemic starting material forms a different product diastereomer in enantioenriched form. This scenario is distinct from a classic kinetic resolution in which one enantiomer reacts significantly faster than the other.<sup>17</sup> While examples of such processes have been reported, they remain relatively rare despite of their significant potential utility. 18,19 The possibility of developing a stereodivergent oxa-Pictet-Spengler reaction with racemic tryptophols was evaluated with (±)-7a, a material that can be readily prepared in one step from indole and the appropriate epoxide (Table1).20 Catalyst 1b provided a promising result, with both diastereomers of product **8a** being obtained with significant ee (entry 1). As we have recently shown that a catalyst with an electron-rich selenourea functionality can outperform the corresponding thiourea catalyst in certain transformations, 21 we were curious to learn whether this exchange could lead to improvements here. Indeed, selenourea-thiourea catalyst 1e provided an

increase in ee for both product diastereomers, without affecting the dr (entry 2). Related catalysts **1f** and **1g** provided no further improvements (entries 3 and 4). Encouragingly, catalyst 1a led to an improvement in diastereoselectivity (entry 5). Under identical conditions at room temperature, selenourea-thiourea catalyst **1h** outperformed **1a** (entry 6). It should be noted that for an ideal stereodivergent process of a racemic mixture, the product dr must be 1:1, with each product diastereomer being formed with identical ee. Since this is not the case in entries 1-6, a kinetic resolution process is operating some extent, leading to less-than-ideal results. Remarkably, upon conducting the reaction at lower concentration at -30 °C, catalyst 1a enabled a stereodivergent reaction with a 1:1 dr. Both diastereomers of 8a were isolated with identical, excellent ee (entry 7). Under these conditions, in contrast to the room temperature experiments, catalyst **1h** provided no further improvements (entry 8).

The scope of the reaction was explored with catalyst 1a (Scheme 4). A range of aromatic aldehydes with variable substituents readily underwent stereospecific oxa-Pictet Spengler reactions with tryptophol (±)-7a. Tryptophols substituted on the indole ring also provided products in good yields and enantioselectivities. In addition, exchange of the phenyl group in (±)-7a with other substituents was tolerated.



**Scheme 5**. Experimental <sup>13</sup>C and <sup>2</sup>H KIEs determined for the reaction of tryptophol and benzaldehyde dimethyl acetal catalyzed by **1a**. Numbers in parenthesis represent the 95% confidence range in the last digit of each KIE as determined from 12 measurements from two independent experiments. The first irreversible step and enantioselectivity-determining step in the catalytic cycle identified from the KIE experiments and DFT calculations are also shown. Energies are Gibbs free energies relative to the oxocarbenium ion-catalyst prereactive complex.

Our next focus was to elucidate the mechanistic details of the title reaction including identifying the origins of

enantioselectivity. Our initial mechanistic experiments (Scheme 3) point towards an oxocarbenium ion mechanism for the asymmetric oxa-Pictet Spengler reaction catalyzed by 1a and 2a•HCl. We sought to probe the rate- and enantioselectivity-determining step within this mechanism using 13C and 2H kinetic isotope effect (KIE) experiments and Two independent reactions of computational studies. tryptophol and benzaldehyde dimethyl acetal in the presence of 5 Å molecular sieves and catalyst 1a + HCl were taken to 72±2% and 80±2% conversion (in tryptophol) and the unreacted tryptophol was re-isolated from the reaction mixture in order to determine <sup>13</sup>C KIEs at natural abundance. The <sup>13</sup>C KIE at the key bond-forming aromatic carbon (C2) of tryptophol is 1.004(3) (Scheme 5). The absence of a significant normal KIE at C2 suggests that C-C bond-formation is not the first irreversible step in the catalytic cycle for tryptophol. To probe whether the first irreversible step occurs before (oxocarbenium ion formation) or after (rearomatization) C-C bond-formation, we conducted competitive  $k_H/k_D$  using a 50:50 mixture of 2-d-tryptophol:tryptophol and measured a  $k_{\rm H}/k_{\rm D}$  of 1.0±0.1 (Scheme 5). This unity  $k_{\rm H}/k_{\rm D}$  value excludes rearomatization as the first irreversible step in the catalytic cycle for tryptophol. Taken together, the <sup>13</sup>C and <sup>2</sup>H KIE experiments provide strong support for oxocarbenium ion formation as the first irreversible step in the catalytic cycle for tryptophol.

Next, we turned to DFT calculations to identify which of the two steps following oxocarbenium ion formation - C-C bondformation or rearomatization - is the enantioselectivitydetermining step (has the higher barrier) in the catalytic cycle. Accordingly, we identified the lowest energy transition state for C–C bond-formation leading to the major enantiomer (*R*) of product (TS<sub>CC-R</sub>). Following C-C bond-formation, we modeled the rearomatization of indole ring via deprotonation using one of the sulfur atoms of the catalyst  $(TS_{depi-R})$  or the bound chloride ion  $(TS_{dep2-R})$  as well as potential bases (not shown, See SI). The key findings from these calculations were (a)  $TS_{dep_1-R}$  is the preferred pathway for rearomatization since it was found to be 3.6 kcal/mol lower in energy than TS<sub>dep2-R,<sup>22</sup></sub> and (b)  $TS_{CC-R}$  is 3.2 kcal/mol higher in energy ( $\Delta G^{\ddagger}=7.3$ kcal/mol relative to the pre-reactive complex, Scheme 5) than  $TS_{depi-R}$  ( $\Delta G^{\ddagger}=4.1$  kcal/mol relative to the pre-reactive complex, Scheme 5). Therefore, our computational studies suggest that C-C bond-formation is the enantioselectivitydetermining step in the catalytic cycle.

Origin of enantioselectivity: Having identified C-C bondformation as the enantioselectivity-determining step in the catalytic cycle, we conducted a thorough examination<sup>22</sup> of the C-C bond-forming transition state leading to both enantiomers of product 3a (Figure 2A). As mentioned earlier,  $TS_{CC-R}$  is the lowest-energy TS leading to the R-enantiomer of 3a - this TS was found to be 2.6 kcal/mol lower in energy than the lowest-energy TS leading to the S-enantiomer of 3a (TS<sub>CC</sub>s), which is in reasonable agreement with the experimental 91% ee ( $\Delta\Delta G^{\ddagger}$ =1.6 kcal/mol). A visual analysis of the two transition structures (Figure 2) shows that these TSs are stabilized by near-identical stabilizing interactions, namely (a) a strong H-bonding interaction between the indole NH and the thiourea-bound chloride anion (2.1 Å in both TSs) and (b) a non-conventional H-bonding interaction between the oxocarbenium C-H and the sulfur atom in the catalyst arm with the dicyclooctyl amine moieties (2.61 Å in  $TS_{CC-R}$  and 2.68 Å in  $TS_{CC-S}$ . The origin of the energy difference between  $TS_{CC-R}$  and  $TS_{CC-S}$  is not immediately obvious from this analysis and so we turned to a more detailed energy decomposition analysis as described below.

To understand the origin of enantioselectivity, we chose to decompose the lowest-lying TS energies leading to the major enantiomers minor using distortioninteraction/activation-strain approach.<sup>23–26</sup> Decomposing the TS energy revealed that the catalyst fragments suffer from identical distortions (as shown in figure 2C) in both the TSs (only slightly favoring the major enantiomeric TS by 0.3 kcal/mol). Evaluating the electrostatic component of the interaction energy revealed only a minor electrostatic stabilization of the TS leading to the major enantiomer (0.5 kcal/mol) compared to the minor enantiomeric TS suggesting that increasing the electrostatic stabilization will likely erode selectivity.<sup>22,27,28</sup> Furthermore, as dispersion interactions are known to play a key role in these systems, we employed Grimme's DFTD3 code<sup>29,30</sup> coupled with Becke-Johnson corrections, to evaluate the dispersion component of the interaction energy. This analysis revealed that TS<sub>CC-R</sub> enjoys favorable dispersion interactions compared to TS<sub>CC-S</sub> by 1.9 kcal/mol. Independent gradient model with Hirschfeld partitioning (IGMH)31 was employed to visualize the noncovalent interactions at play in the enantiomeric TSs. Comparison of the green surfaces in Figure 2B, which represent weak Van der Waal's interactions at play in these systems, shows that TS<sub>CC-R</sub> enjoys more favorable Van der Waal's interactions compared to TS<sub>CC-S</sub> - further supporting the results from D<sub>3</sub> computations. These results provide strong support for dispersion interactions being the main origin of enantioselectivity in these systems.

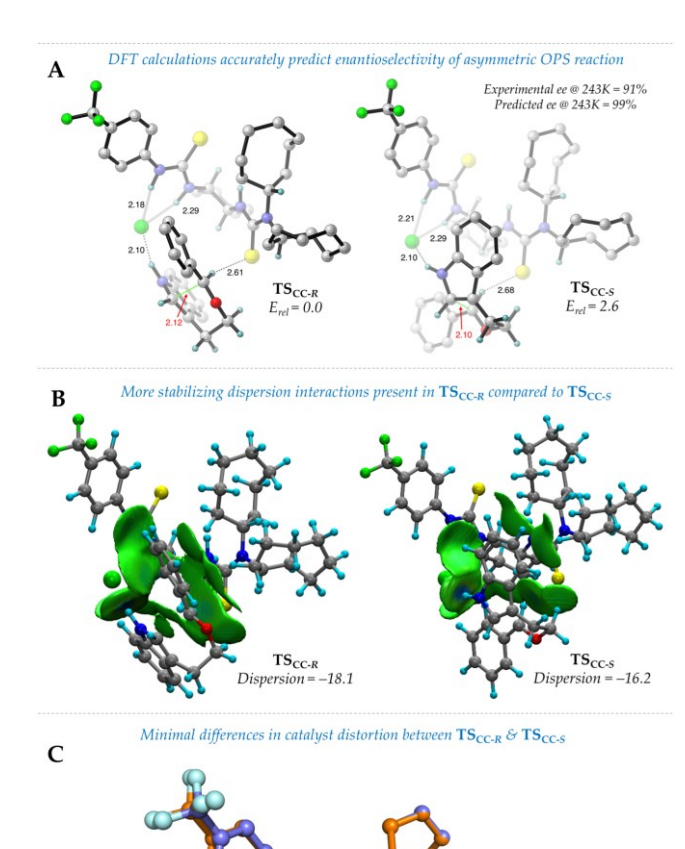


**Figure 2**. (A)Transition state geometries for C–C bondformation leading to the major (*R*) and minor (*S*) enantiomer of **3a**. All distances are in angstroms (Å) and energies are in kcal/mol. Most hydrogen atoms have been removed for clarity. (B) Independent gradient model with Hirschfeld partitioning to visualize the numerous non-covalent interactions present in these systems. Green surfaces

correspond to weak Van der Waal's interactions present in the

system. (C) An overlay of the catalysts fragments from TS

leading to major and minor enantiomers.

Finally using the TS models in Figure 2A as template for predicting enantioselectivity, we modeled transition structures leading to all possible diastereomers in the stereodivergent reaction forming product  $\bf 8a$ . As expected, the presence of a phenyl group at the benzylic position of tryptophol does not impact stereocontrol at the newly-formed stereogenic center and the high enantioselectivity is faithfully translated to both diastereomers ( $\Delta\Delta G^{\ddagger}$ =2.9 kcal/mol for  $\bf TS_{CC-R,R}$  versus  $\bf TS_{CC-S,S}$  and  $\Delta\Delta G^{\ddagger}$ =3.3 kcal/mol for  $\bf TS_{CC-R,S}$  versus  $\bf TS_{CC-S,R}$ ). Moreover, the relative energies of the TSs leading to the major enantiomer of each diastereomer (Figure3,  $\bf TS_{CC-R,R}$  versus  $\bf TS_{CC-R,S}$ ) is only 0.5 kcal/mol – consistent with the 1:1 d.r. observed in the reaction.

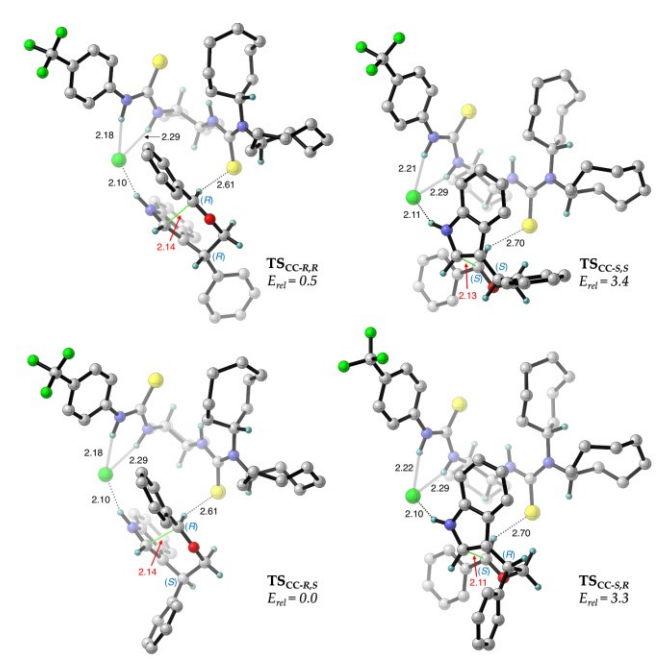


**Figure 3.** (A)Transition state geometries for C–C bond-formation leading all four diastereomers of **8a**. All distances are in angstroms (Å) and energies are in kcal/mol. Most hydrogen atoms have been removed for clarity.

In conclusion, we have conducted a detailed mechanistic analysis of a catalytic enantioselective oxa-Pictet Spengler reaction. In addition to confirming the intermediacy of oxocarbenium ions and ruling out an alternative azafulvenium pathway, <sup>13</sup>C and <sup>2</sup>H KIE experiments revealed oxocarbenium ion formation as the first irreversible step in the catalytic cycle. DFT calculations established C-C bond-formation as the enantioselectivity-determining step, in addition to providing important insights into the role of the key bisthiourea catalysts and its interactions with the oxocarbenium ion and the chloride counter anion. Favorable dispersion interactions, which are less pronounced in the TS leading to the minor enantiomer, were found to be the main origin of enantioselectivity. Our findings were applied to the development of a stereodivergent variant of the oxa-Pictet Spengler reaction with racemic tryptophol derivatives, providing rapid access to stereochemically tetrahydropyrano[3,4-b]indoles in highly enantioenriched form.

#### **AUTHOR INFORMATION**

**Corresponding Author** 

- \* seidel@chem.ufl.edu
- \* vetticatt@binghamton.edu

Notes

The authors declare no competing financial interests.

#### ASSOCIATED CONTENT

Supporting Information

Experimental procedures and characterization data, including X-ray crystal structure of product **8e**. This material is available free of charge via the Internet at http://pubs.acs.org.

#### **ACKNOWLEDGMENTS**

This material is based upon work supported by the National Science Foundation under CHE-1856613 and CHE-2154292 (grants to D.S.) We also acknowledge the National Science Foundation (grant# 1828064 to K.A.A.) and the University of Florida for funding the purchase of the X-ray equipment. Mass spectrometry instrumentation was supported by a grant from the NIH (S10 OD021758-01A1). Research reported in this publication was further supported by the National Institutes of Health under R35 GM145320 (M.J.V.) and by the Office Of The Director of the National Institutes of Health under Award Number S10OD026746. M.J.V. and M.S.C acknowledge support from the XSEDE Science Gateways Program (allocation IDs CHE160009 and CHE210031), which is supported by the National Science Foundation grant number ACI-1548562.

#### REFERENCES

- (1) Selected reviews on the oxa-Pictet-Spengler reaction: (a) Larghi, E. L.; Kaufman, T. S., The oxa-Pictet-Spengler cyclization: Synthesis of isochromans and related pyran-type heterocycles. Synthesis 2006, 187-220; (b) Larghi, E. L.; Kaufman, T. S., Synthesis of Oxacycles Employing the Oxa-Pictet-Spengler Reaction: Recent Developments and New Prospects. Eur. J. Org. Chem. 2011, 2011, 5195-5231; (c) Zhu, Z.; Adili, A.; Zhao, C.; Seidel, D., Catalytic Enantioselective Approaches to the oxa-Pictet-Spengler Cyclization and Other 3,6-Dihydropyran-Forming Reactions. SynOpen 2019, 03, 77-90.
- (2) (a) Buschmann, H.; Michel, R. Verfahren zur Herstellung von Isochromanen. German Patent 614461, 1935; (b) Buschmann, H.; Michel, R. Verfahren zur Herstellung von Isochromanen, Zusatz. German Patent 617646, 1935.
- (a) Doyle, A. G., Ph.D. Thesis, Harvard University, Cambridge. 2008, 267-293; (b) Lombardo, V. M.; Thomas, C. D.; Scheidt, K. A., A Tandem Isomerization/Prins Strategy: Iridium(III)/Brønsted Acid Cooperative Catalysis. Angew. Chem. Int. Ed. 2013, 52, 12910-12914; (c) Ascic, E.; Ohm, R. G.; Petersen, R.; Hansen, M. R.; Hansen, C. L.; Madsen, D.; Tanner, D.; Nielsen, T. E., Synthesis of Oxacyclic Scaffolds via Dual Ruthenium Hydride/Brønsted Acid-Catalyzed Isomerization/Cyclization of Allylic Ethers. Chem. Eur. J. 2014, 20, 3297-3300; (d) Zhao, C.; Chen, S. B.; Seidel, D., Direct Formation of Oxocarbenium Ions under Weakly Acidic Conditions: Catalytic Enantioselective Oxa-Pictet-Spengler Reactions. J. Am. Chem. Soc. 2016, 138, 9053-9056; (e) Das, S.; Liu, L.; Zheng, Y.; Alachraf, M. W.; Thiel, W.; De, C. K.; List, B., Nitrated Confined Imidodiphosphates Enable a Catalytic Asymmetric Oxa-Pictet-Spengler Reaction. J. Am. Chem. Soc. 2016, 138, 9429-9432; (f) Maskeri, M. A.; O'Connor, M. J.; Jaworski, A. A.; Davies, A. V.; Scheidt, K. A., A Cooperative Hydrogen Bond Donor-Brønsted Acid System for the Enantioselective Synthesis of Tetrahydropyrans. Angew. Chem. Int. Ed. 2018, 57, 17225-17229; (g) Zhu, Z.; Odagi, M.; Zhao, C.; Abboud, K. A.; Kirm, H. U.; Saame, J.; Lõkov, M.; Leito, I.; Seidel, D., Highly Acidic Conjugate-Base-Stabilized Carboxylic Acids Catalyze Enantioselective oxa-Pictet-Spengler Reactions with Ketals. Angew. Chem. Int. Ed. 2020, 59, 2028-2032; (h) Maskeri, M. A.; Brueckner, A. C.; Feoktistova, T.; O'Connor, M. J.; Walden, D. M.; Cheong, P. H.-Y.; Scheidt, K. A., Mechanism and origins of selectivity in the enantioselective oxa-Pictet-Spengler reaction: a cooperative catalytic complex from a hydrogen bond donor and chiral phosphoric acid. Chem. Sci. 2020, 11, 8736-8743; (i) Riegel, G. F.; Payne, C.; Kass, S. R., Effects of Brønsted acid cocatalysts on the activities and selectivities of charge-enhanced thiourea organocatalysts in Friedel-Crafts and oxa-Pictet-Spengler reactions. J. Phys. Org. Chem. 2022, e4321.
- (4) Selected recent reviews on the Pictet–Spengler reaction: (a) Stöckigt, J.; Antonchick, A. P.; Wu, F. R.; Waldmann, H., The Pictet–Spengler Reaction in Nature and in Organic Chemistry. *Angew. Chem. Int. Ed.* **2011**, 50, 8538-8564; (b) Ingallina, C.; D'Acquarica, I.; Delle Monache, G.; Ghirga, F.; Quaglio, D.; Ghirga, P.; Berardozzi, S.;

- Markovic, V.; Botta, B., The Pictet-Spengler Reaction Still on Stage. *Curr. Pharm. Design* 2016, 22, 1808-1850; (c) Calcaterra, A.; Mangiardi, L.; Delle Monache, G.; Quaglio, D.; Balducci, S.; Berardozzi, S.; Iazzetti, A.; Franzini, R.; Botta, B.; Ghirga, F., The Pictet-Spengler Reaction Updates Its Habits. *Molecules* 2020, 25, 414; (d) Glinsky-Olivier, N.; Guinchard, X., Enantioselective Catalytic Methods for the Elaboration of Chiral Tetrahydro-β-carbolines and Related Scaffolds. *Synthesis* 2017, 49, 2605-2620; (e) Gholamzadeh, P., Chapter Three The Pictet-Spengler Reaction: A Powerful Strategy for the Synthesis of Heterocycles. In *Adv. Heterocycl. Chem.*, Scriven, E. F. V.; Ramsden, C. A., Eds. Academic Press: 2019; Vol. 127, pp 153-226; (f) Zheng, C.; You, S.-L., Exploring the Chemistry of Spiroindolenines by Mechanistically-Driven Reaction Development: Asymmetric Pictet-Spengler-type Reactions and Beyond. *Acc. Chem. Res.* 2020, 53, 974-987.
- (5) Selected reviews covering aspects of catalytic enantioselective reactions involving oxocarbenium ions: (a) Moyano, A.; Rios, R., Asymmetric Organocatalytic Cyclization and Cycloaddition Reactions. Chem. Rev. 2011, 111, 4703-4832; (b) Gualandi, A.; Rodeghiero, G.; Cozzi, P. G., Catalytic Stereoselective SN1-Type Reactions Promoted by Chiral Phosphoric Acids as Brønsted Acid Catalysts. Asian J. Org. Chem. 2018, 7, 1957-1981; (c) Tamanna; Kumar, M.; Joshi, K.; Chauhan, P., Catalytic Asymmetric Synthesis of Isochroman Derivatives. Adv. Synth. Catal. 2020, 362, 1907-1926; (d) Liu, J.; Dasgupta, S.; Watson, M. P., Enantioselective additions of copper acetylides to cyclic iminium and oxocarbenium ions. Beilstein J. Org. Chem. 2015, 11, 2696-2706; (e) Lei, C.-W.; Mu, B.-S.; Zhou, F.; Yu, J.-S.; Zhou, Y.; Zhou, J., Organocatalytic enantioselective reactions involving prochiral carbocationic intermediates. Chem. Commun. **2021,** 57, 9178-9191. See also reference 1c.
- Examples of catalytic enantioselective reactions involving the intermediacy of oxocarbenium ions: (a) Braun, M.; Kotter, W., Titanium(IV)-Catalyzed Dynamic Kinetic Asymmetric Transformation of Alcohols, Silyl Ethers, and Acetals under Carbon Allylation. Angew. Chem. Int. Ed. 2004, 43, 514-517; (b) Umebayashi, N.; Hamashima, Y.; Hashizume, D.; Sodeoka, M., Catalytic Enantioselective Aldol-type Reaction of β-Ketosters with Acetals. Angew. Chem. Int. Ed. 2008, 47, 4196-4199; (c) Reisman, S. E.; Doyle, A. G.; Jacobsen, E. N., Enantioselective Thiourea-Catalyzed Additions to Oxocarbenium Ions. J. Am. Chem. Soc. 2008, 130, 7198-7199; (d) Terada, M.; Tanaka, H.; Sorimachi, K., Enantioselective Direct Aldol-Type Reaction of Azlactone via Protonation of Vinyl Ethers by a Chiral Bronsted Acid Catalyst. J. Am. Chem. Soc. 2009, 131, 3430-3431; (e) Moquist, P. N.; Kodama, T.; Schaus, S. E., Enantioselective Addition of Boronates to Chromene Acetals Catalyzed by a Chiral Brønsted Acid/Lewis Acid System. Angew. Chem. Int. Ed. 2010, 49, 7096-7100; (f) Čorić, I.; Vellalath, S.; List, B., Catalytic Asymmetric Transacetalization. J. Am. Chem. Soc. 2010, 132, 8536-8537; (g) Maity, P.; Srinivas, H. D.; Watson, M. P., Copper-Catalyzed Enantioselective Additions to Oxocarbenium Ions: Alkynylation of Isochroman Acetals. J. Am. Chem. Soc. 2011, 133, 17142-17145; (h) Coric, I.; List, B., Asymmetric spiroacetalization catalysed by confined Bronsted acids. Nature 2012, 483, 315-319; (i) Rueping, M.; Volla, C. M. R.; Atodiresei, I., Catalytic Asymmetric Addition of Aldehydes to Oxocarbenium Ions: A Dual Catalytic System for the Synthesis of Chromenes. Org. Lett. 2012, 14, 4642-4645; (j) Sun, Z.; Winschel, G. A.; Borovika, A.; Nagorny, P., Chiral Phosphoric Acid-Catalyzed Enantioselective and Diastereoselective Spiroketalizations. J. Am. Chem. Soc. 2012, 134, 8074-8077; (k) Kim, J. H.; Čorić, I.; Vellalath, S.; List, B., The Catalytic Asymmetric Acetalization. Angew. Chem. Int. Ed. 2013, 52, 4474-4477; (l) Meng, Z.; Sun, S.; Yuan, H.; Lou, H.; Liu, L., Catalytic Enantioselective Oxidative Cross-Coupling of Benzylic Ethers with Aldehydes. Angew. Chem. Int. Ed. 2014, 53, 543-547; (m) Dasgupta, S.; Rivas, T.; Watson, M. P., Enantioselective Copper(I)-Catalyzed Alkynylation of Oxocarbenium Ions to Set Diaryl Tetrasubstituted Stereocenters. Angew. Chem. Int. Ed. 2015, 54, 14154-14158; (n) Qian, H.; Zhao, W.; Wang, Z.; Sun, J., Organocatalytic Enantio- and Diastereoselective Synthesis of 1,2-Dihydronaphthalenes from Isobenzopyrylium Ions. J. Am. Chem. Soc. 2015, 137, 560-563; (o) Gheewala, C. D.; Collins, B. E.; Lambert, T. H., An aromatic ion platform for enantioselective Brønsted acid catalysis. Science 2016,

351, 961-965; (p) Liu, L.; Kaib, P. S. J.; Tap, A.; List, B., A General Catalytic Asymmetric Prins Cyclization. J. Am. Chem. Soc. 2016, 138, 10822-10825; (q) Hardman-Baldwin, A. M.; Visco, M. D.; Wieting, J. M.; Stern, C.; Kondo, S.-i.; Mattson, A. E., Silanediol-Catalyzed Chromenone Functionalization. Org. Lett. 2016, 18, 3766-3769; (r) Wu, H.; Wang, Q.; Zhu, J., Organocatalytic Enantioselective Acyloin Rearrangement of α-Hydroxy Acetals to α-Alkoxy Ketones. Angew. Chem. Int. Ed. 2017, 56, 5858-5861; (s) Lee, S.; Kaib, P. S. J.; List, B., Asymmetric Catalysis via Cyclic, Aliphatic Oxocarbenium Ions. J. Am. Chem. Soc. 2017, 139, 2156-2159; (t) Fischer, T.; Bamberger, J.; Gómez-Martínez, M.; Piekarski, D. G.; García Mancheño, O., Helical Multi-Coordination Anion-Binding Catalysts for the Highly Enantioselective Dearomatization of Pyrylium Derivatives. Angew. Chem. Int. Ed. 2019, 58, 3217-3221; (u) DeRatt, L. G.; Pappoppula, M.; Aponick, A., A Facile Enantioselective Alkynylation of Chromones. Angew. Chem. Int. Ed. 2019, 58, 8416-8420; (v) Pan, Y.-L.; Zheng, H.-L.; Wang, J.; Yang, C.; Li, X.; Cheng, J.-P., Enantioselective Allylation of Oxocarbenium Ions Catalyzed by Bi(OAc)3/Chiral Phosphoric Acid. ACS Catal. 2020, 10, 8069-8076; (w) Zhu, Z.; Odagi, M.; Supantanapong, N.; Xu, W.; Saame, J.; Kirm, H.-U.; Abboud, K. A.; Leito, I.; Seidel, D., Modular Design of Chiral Conjugate-Base-Stabilized Carboxylic Acids: Catalytic Enantioselective [4 + 2] Cycloadditions of Acetals. J. Am. Chem. Soc. 2020, 142, 15252-15258; (x) Yang, T.; Sun, Y.; Wang, H.; Lin, Z.; Wen, J.; Zhang, X., Iridium-Catalyzed Enantioselective Hydrogenation of Oxocarbenium Ions: A Case of Ionic Hydrogenation. Angew. Chem. Int. Ed. 2020, 59, 6108-6114; (y) Kutateladze, D. A.; Jacobsen, E. N., Cooperative Hydrogen-Bond-Donor Catalysis with Hydrogen Chloride Enables Highly Enantioselective Prins Cyclization Reactions. J. Am. Chem. Soc. 2021, 143, 20077-20083; (z) Zhou, L.; Jia, K.; Liu, X.; Liu, L., Enantioselective Transfer Hydrogenation of Oxocarbenium Ions Enables Asymmetric Access to α-Substituted 1,3-Dihydroisobenzofurans. Synthesis 2022, 54, 421-428.

Selected reviews on dual catalysis: (a) Piovesana, S.; (7) Scarpino Schietroma, D. M.; Bella, M., Multiple Catalysis with Two Chiral Units: An Additional Dimension for Asymmetric Synthesis. Angew. Chem., Int. Ed. 2011, 50, 6216-6232; (b) Allen, A. E.; MacMillan, D. W. C., Synergistic catalysis: A powerful synthetic strategy for new reaction development. Chem. Sci. 2012, 3, 633-658; (c) Wende, R. C.; Schreiner, P. R., Evolution of asymmetric organocatalysis: multi- and retrocatalysis. Green Chem. 2012, 14, 1821-1849; (d) Brière, J.-F.; Oudeyer, S.; Dalla, V.; Levacher, V., Recent advances in cooperative ion pairing in asymmetric organocatalysis. Chem. Soc. Rev. 2012, 41, 1696-1707; (e) Inamdar, S. M.; Shinde, V. S.; Patil, N. T., Enantioselective cooperative catalysis. Org. Biomol. Chem. 2015, 13, 8116-8162; (f) Mitra, R.; Niemeyer, J., Dual Brønsted acid Organocatalysis: Cooperative Asymmetric Catalysis with Combined Phosphoric and Carboxylic Acids. ChemCatChem 2018, 10, 1221-1234; (g) Romiti, F.; del Pozo, J.; Paioti, P. H. S.; Gonsales, S. A.; Li, X.; Hartrampf, F. W. W.; Hoveyda, A. H., Different Strategies for Designing Dual-Catalytic Enantioselective Processes: From Fully Cooperative to Non-cooperative Systems. J. Am. Chem. Soc. 2019, 141, 17952-17961; (h) Sinibaldi, A.; Nori, V.; Baschieri, A.; Fini, F.; Arcadi, A.; Carlone, A., Organocatalysis and Beyond: Activating Reactions with Two Catalytic Species. Catalysts 2019, 9, 928; (i) Xiao, X.; Shao, B.-X.; Lu, Y.-J.; Cao, Q.-Q.; Xia, C.-N.; Chen, F.-E., Recent Advances in Asymmetric Organomulticatalysis. Adv. Synth. Catal. 2021, 363, 352-387.

(8) Selected reviews on iminium catalysis: (a) Lelais, G.; MacMillan, D. W. C., Modern strategies in organic catalysis: The advent and development of iminium activation. *Aldrichimica Acta* **2006**, 39, 79–87; (b) Erkkilae, A.; Majander, I.; Pihko, P. M., Iminium Catalysis. *Chem. Rev.* **2007**, 107, 5416–5470; (c) Brazier, J. B.; Tomkinson, N. C. O., Secondary and Primary Amine Catalysts for Iminium Catalysis. In *Asymmetric Organocatalysis*, List, B., Ed. Springer Berlin Heidelberg: Berlin, Heidelberg, 2010; pp 281-347. Seminal studies: (d) Ahrendt, K. A.; Borths, C. J.; MacMillan, D. W. C., New Strategies for Organic Catalysis: The First Highly Enantioselective Organocatalytic Diels-Alder Reaction. *J. Am. Chem. Soc.* **2000**, 122, 4243–4244; (e) Jen, W. S.; Wiener, J. J. M.; MacMillan, D. W. C., New Strategies for Organic Catalysis: The First Enantioselective

Organocatalytic 1,3-Dipolar Cycloaddition. J. Am. Chem. Soc. 2000, 122, 9874–9875.

(9) For seminal examples of iminium catalysis with intrinsically chiral counter anions, see: (a) Mayer, S.; List, B., Asymmetric counteranion-directed catalysis. *Angew. Chem. Int. Ed.* **2006**, *45*, 4193–4195; (b) Wang, X.; List, B., Asymmetric counteranion-directed catalysis for the epoxidation of enals. *Angew. Chem. Int. Ed.* **2008**, *47*, 1119–1122.

(10)Examples of asymmetric catalysis in which turnover is achieved by elimination of an amine catalyst: (a) Xu, D. Q.; Wang, Y. F.; Luo, S. P.; Zhang, S.; Zhong, A. G.; Chen, H.; Xu, Z. Y., A Novel Enantioselective Catalytic Tandem Oxa-Michael-Henry Reaction: One-Pot Organocatalytic Asymmetric Synthesis of 3-Nitro-2Hchromenes. Adv. Synth. Catal. 2008, 350, 2610-2616; (b) Wang, Y.-F.; Zhang, W.; Luo, S.-P.; Li, B.-L.; Xia, A.-B.; Zhong, A.-G.; Xu, D.-Q., One-Pot Organocatalytic Asymmetric Synthesis of 3-Nitro-1,2dihydroquinolines by a Dual-Activation Protocol. Chem. Asian J. 2009, 4, 1834-1838; (c) Lee, A.; Michrowska, A.; Sulzer-Mosse, S.; List, B., The Catalytic Asymmetric Knoevenagel Condensation. Angew. Chem. Int. Ed. 2011, 50, 1707-1710; (d) Yin, G.; Zhang, R.; Li, L.; Tian, J.; Chen, L., One-Pot Enantioselective Synthesis of 3-Nitro-2Hchromenes Catalyzed by a Simple 4-Hydroxyprolinamide with 4-Nitrophenol as Cocatalyst. Eur. J. Org. Chem. 2013, 2013, 5431-5438; (e) Luo, H.; Yan, X.; Chen, L.; Li, Y.; Liu, N.; Yin, G., Enantioselective Catalytic Domino Aza-Michael-Henry Reactions: One-Pot Asymmetric Synthesis of 3-Nitro-1,2-dihydroquinolines via Iminium Activation. Eur. J. Org. Chem. 2016, 2016, 1702-1707.

Selected reviews on anion-binding catalysis and catalysis with chiral anions: (a) Lacour, J.; Hebbe-Viton, V., Recent developments in chiral anion mediated asymmetric chemistry. Chem. Soc. Rev. 2003, 32, 373-382; (b) Lacour, J.; Moraleda, D., Chiral anionmediated asymmetric ion pairing chemistry. Chem. Commun. 2009, 7073-7089; (c) Zhang, Z.; Schreiner, P. R., (Thio)urea organocatalysis - What can be learnt from anion recognition? Chem. Soc. Rev. 2009, 38, 1187-1198; (d) Beckendorf, S.; Asmus, S.; Mancheño, O. G., H-Donor Anion Acceptor Organocatalysis-The Ionic Electrophile Activation Approach. ChemCatChem 2012, 4, 926-936; (e) Avila, E. P.; Amarante, G. W., Recent Advances in Asymmetric Counteranion-directed Catalysis (ACDC). ChemCatChem 2012, 4, 1713-1721; (f) Phipps, R. J.; Hamilton, G. L.; Toste, F. D., The progression of chiral anions from concepts to applications in asymmetric catalysis. Nat. Chem. 2012, 4, 603-614; (g) Woods, P. A.; Smith, A. D., Supramolecular organocatalysis. Supramolecular Chemistry: From Molecules to Nanomaterials 2012, 4, 1383-1414; (h) Mahlau, M.; List, B., Asymmetric Counteranion-Directed Catalysis: Concept, Definition, Applications. Angew. Chem. Int. Ed. 2013, 52, 518-533; (i) Brak, K.; Jacobsen, E. N., Asymmetric Ion-Pairing Catalysis. Angew. Chem. Int. Ed. 2013, 52, 534-561; (j) Seidel, D., The Anion-Binding Approach to Catalytic Enantioselective Acyl Transfer. Synlett 2014, 25, 783-794; (k) Busschaert, N.; Caltagirone, C.; Van Rossom, W.; Gale, P. A., Applications of Supramolecular Anion Recognition. Chem. Rev. 2015, 115, 8038-8155; (l) Visco, M. D.; Attard, J.; Guan, Y.; Mattson, A. E., Anion-binding catalyst designs for enantioselective synthesis. Tetrahedron Lett. 2017, 58, 2623-2628; (m) Schifferer, L.; Stinglhamer, M.; Kaur, K.; Macheño, O. G., Halides as versatile anions in asymmetric anion-binding organocatalysis. Beilstein J. Org. Chem. 2021, 17, 2270-2286; (n) Entgelmeier, L.-M.; Mancheño, O. G., Activation Modes in Asymmetric Anion-Binding Catalysis. Synthesis 2022, 54, 3907-3927.

(12) Examples of catalytic reactions likely to involve chloride anion recognition: (a) Taylor, M. S.; Jacobsen, E. N., Highly enantioselective catalytic acyl-Pictet-Spengler reactions. *J. Am. Chem. Soc.* **2004**, *126*, 10558–10559; (b) Taylor, M. S.; Tokunaga, N.; Jacobsen, E. N., Enantioselective thiourea-catalyzed acyl-mannich reactions of isoquinolines. *Angew. Chem. Int. Ed.* **2005**, *44*, 6700–6704; (c) Raheem, I. T.; Thiara, P. S.; Peterson, E. A.; Jacobsen, E. N., Enantioselective Pictet-Spengler-Type Cyclizations of Hydroxylactams: H-Bond Donor Catalysis by Anion Binding. *J. Am. Chem. Soc.* **2007**, *129*, 13404–13405; (d) Yamaoka, Y.; Miyabe, H.; Takemoto, Y., Catalytic enantioselective petasis-type reaction of quinolines catalyzed by a newly designed thiourea catalyst. *J. Am.* 

Chem. Soc. 2007, 129, 6686-+; (e) Martínez-García, H.; Morales, D.; Pérez, J.; Coady, D. J.; Bielawski, C. W.; Gross, D. E.; Cuesta, L.; Marquez, M.; Sessler, J. L., Calix[4]pyrrole as a Promoter of the CuCl-Catalyzed Reaction of Styrene and Chloramine-T. Organometallics 2007, 26, 6511-6514; (f) Peterson, E. A.; Jacobsen, E. N., Enantioselective, Thiourea-Catalyzed Intermolecular Addition of Indoles to Cyclic N-Acyl Iminium Ions. Angew. Chem. Int. Ed. 2009, 48, 6328-6331; (g) Knowles, R. R.; Lin, S.; Jacobsen, E. N., Enantioselective Thiourea-Catalyzed Cationic Polycyclizations. J. Am. Chem. Soc. 2010, 132, 5030-5032; (h) Schafer, A. G.; Wieting, J. M.; Fisher, T. J.; Mattson, A. E., Chiral Silanediols in Anion-Binding Catalysis. Angew. Chem. Int. Ed. 2013, 11321-11324; (i) Zhao, Q.; Wen, J.; Tan, R.; Huang, K.; Metola, P.; Wang, R.; Anslyn, E. V.; Zhang, X., Rhodium-Catalyzed Asymmetric Hydrogenation of Unprotected NH Imines Assisted by a Thiourea. Angew. Chem. Int. Ed. 2014, 53, 8467-8470; (j) Zhang, H.; Lin, S.; Jacobsen, E. N., Enantioselective Selenocyclization via Dynamic Kinetic Resolution of Seleniranium Ions by Hydrogen-Bond Donor Catalysts. J. Am. Chem. Soc. 2014, 136, 16485-16488; (k) Zurro, M.; Asmus, S.; Beckendorf, S.; Mück-Lichtenfeld, C.; García Mancheño, O., Chiral Helical Oligotriazoles: New Class of Anion-Binding Catalysts for the Asymmetric Dearomatization of Electron-Deficient N-Heteroarenes. J. Am. Chem. Soc. 2014, 136, 13999-14002; (1) García Mancheño, O.; Asmus, S.; Zurro, M.; Fischer, T., Highly Enantioselective Nucleophilic Dearomatization of Pyridines by Anion-Binding Catalysis. Angew. Chem. Int. Ed. 2015, 54, 8823-8827; (m) Shirakawa, S.; Liu, S.; Kaneko, S.; Kumatabara, Y.; Fukuda, A.; Omagari, Y.; Maruoka, K., Tetraalkylammonium Salts as Hydrogen-Bonding Catalysts. Angew. Chem. Int. Ed. 2015, 54, 15767-15770; (n) Jungbauer, S. H.; Huber, S. M., Cationic Multidentate Halogen-Bond Donors in Halide Abstraction Organocatalysis: Catalyst Optimization by Preorganization. J. Am. Chem. Soc. 2015, 137, 12110-12120; (o) Ford, D. D.; Lehnherr, D.; Kennedy, C. R.; Jacobsen, E. N., Anion-Abstraction Catalysis: The Cooperative Mechanism of α-Chloroether Activation by Dual Hydrogen-Bond Donors. ACS Catal. 2016, 6, 4616-4620; (p) Ray Choudhury, A.; Mukherjee, S., Enantioselective dearomatization of isoquinolines by anion-binding catalysis en route to cyclic [small alpha]-aminophosphonates. Chem. Sci. 2016, 7, 6940-6945; (q) Wen, J.; Tan, R.; Liu, S.; Zhao, Q.; Zhang, X., Strong Bronsted acid promoted asymmetric hydrogenation of isoquinolines and quinolines catalyzed by a Rh-thiourea chiral phosphine complex via anion binding. Chem. Sci. 2016, 7, 3047-3051; (r) Park, Y.; Schindler, C. S.; Jacobsen, E. N., Enantioselective Aza-Sakurai Cyclizations: Dual Role of Thiourea as H-Bond Donor and Lewis Base. J. Am. Chem. Soc. 2016, 138, 14848-14851; (s) Ford, D. D.; Lehnherr, D.; Kennedy, C. R.; Jacobsen, E. N., On- and Off-Cycle Catalyst Cooperativity in Anion-Binding Catalysis. J. Am. Chem. Soc. 2016, 138, 7860-7863; (t) Zhao, C.; Sojdak, C. A.; Myint, W.; Seidel, D., Reductive Etherification via Anion-Binding Catalysis. J. Am. Chem. Soc. 2017, 139, 10224-10227; (u) Park, Y.; Harper, K. C.; Kuhl, N.; Kwan, E. E.; Liu, R. Y.; Jacobsen, E. N., Macrocyclic bis-thioureas catalyze stereospecific glycosylation reactions. Science 2017, 355, 162-166; (v) Bendelsmith, A. J.; Kim, S. C.; Wasa, M.; Roche, S. P.; Jacobsen, E. N., Enantioselective Synthesis of α-Allyl Amino Esters via Hydrogen-Bond-Donor Catalysis. J. Am. Chem. Soc. 2019, 141, 11414-11419; (w) Dorel, R.; Feringa, B. L., Stereodivergent Anion Binding Catalysis with Molecular Motors. Angew. Chem. Int. Ed. 2020, 59, 785-789; (x) Matador, E.; Iglesias-Sigüenza, J.; Monge, D.; Merino, P.; Fernández, R.; Lassaletta, J. M., Enantio- and Diastereoselective Nucleophilic Addition of N-tert-Butylhydrazones to Isoquinolinium Ions through Anion-Binding Catalysis. Angew. Chem. Int. Ed. 2021, 60, 5096-5101; (y) Gómez-Martínez, M.; del Carmen Pérez-Aguilar, M.; Piekarski, D. G.; Daniliuc, C. G.; García Mancheño, O., N,N-Dialkylhydrazones as Versatile Umpolung Reagents in Enantioselective Anion-Binding Catalysis. Angew. Chem. Int. Ed. 2021, 60, 5102-5107. See also references 6c, 6y.

(13) Examples of iminium catalysis involving anion binding: (a) Wang, Y.; Yu, T.-Y.; Zhang, H.-B.; Luo, Y.-C.; Xu, P.-F., Hydrogen-Bond-Mediated Supramolecular Iminium Ion Catalysis. *Angew. Chem. Int. Ed.* **2012**, *51*, 12339-12342; (b) Gu, Y.; Wang, Y.; Yu, T.-Y.; Liang, Y.-M.; Xu, P.-F., Rationally Designed Multifunctional Supramolecular Iminium Catalysis: Direct Vinylogous Michael Addition of

Unmodified Linear Dienol Substrates. *Angew. Chem. Int. Ed.* **2014**, 53, 14128-14131.

(14) Marigo, M.; Wabnitz, T. C.; Fielenbach, D.; Jørgensen, K. A., Enantioselective Organocatalyzed  $\alpha$  Sulfenylation of Aldehydes. *Angew. Chem. Int. Ed.* **2005**, *44*, 794-797.

Examples of reactions in which replacement of indole *N*–H (15) for N-Me leads to dramatically reduced enantioselectivities: (a) Herrera, R. P.; Sgarzani, V.; Bernardi, L.; Ricci, A., Catalytic enantioselective Friedel-Crafts alkylation of indoles with nitroalkenes by using a simple thiourea organocatalyst. Angew. Chem. Int. Ed. 2005, 44, 6576-6579; (b) Jia, Y.-X.; Zhong, J.; Zhu, S.-F.; Zhang, C.-M.; Zhou, Q.-L., Chiral Brønsted Acid Catalyzed Enantioselective Friedel-Crafts Reaction of Indoles and α-Aryl Enamides: Construction of Quaternary Carbon Atoms. *Angew. Chem. Int. Ed.* **2007**, *46*, 5565-5567; (c) Itoh, J.; Fuchibe, K.; Akiyama, T., Chiral phosphoric acid catalyzed enantioselective Friedel-Crafts alkylation of indoles with nitroalkenes: cooperative effect of 3.ANG. molecular sieves. Angew. Chem. Int. Ed. 2008, 47, 4016-4018; (d) Zheng, C.; Sheng, Y.-F.; Li, Y.-X.; You, S.-L., A theoretical investigation into chiral phosphoric acid-catalyzed asymmetric Friedel-Crafts reactions of nitroolefins and 4,7dihydroindoles: reactivity and enantioselectivity. Tetrahedron 2010, 66, 2875-2880; (e) Takashi, H.; Masahiro, Y., DFT Study of Chiral-Phosphoric-Acid-Catalyzed Enantioselective Friedel-Crafts Reaction of Indole with Nitroalkene: Bifunctionality and Substituent Effect of Phosphoric Acid. Chem. Asian. J. 2011, 6, 510-516; (f) Qi, L.-W.; Mao, J.-H.; Zhang, J.; Tan, B., Organocatalytic asymmetric arylation of indoles enabled by azo groups. Nat. Chem. 2018, 10, 58-64; (g) Nakamura, S.; Furukawa, T.; Hatanaka, T.; Funahashi, Y., Enantioselective aza-Friedel-Crafts reaction of cyclic ketimines with indoles using chiral imidazoline-phosphoric acid catalysts. Chem. Commun. 2018, 54, 3811-3814; (h) Odagi, M.; Araki, H.; Min, C.; Yamamoto, E.; Emge, T. J.; Yamanaka, M.; Seidel, D., Insights into the Structure and Function of a Chiral Conjugate-Base-Stabilized Brønsted Acid Catalyst. Eur. J. Org. Chem. 2019, 2019, 486-492. See

(16) When an otherwise identical experiment was conducted with acetophenone dimethyl ketal, the corresponding oxa-Pictet-Spengler product containing a tetrasubstituted stereogenic center was obtained in 74% yield and 10% ee, following a reaction time of two hours. For an efficient variant of this reaction catalyzed by a different chiral Brønsted acid catalyst, see reference 3g.

(17) Min, C.; Seidel, D., Stereochemically Rich Polycyclic Amines from the Kinetic Resolution of Indolines through Intramolecular Povarov Reactions. *Chem. Eur. J.* 2016, 22, 10817-10820. (18) Selected reviews on stereodivergent reactions: (a) Miller, L. C.; Sarpong, R., Divergent reactions on racemic mixtures. *Chem. Soc. Rev.* 2011, 40, 4550-4562; (b) Bihani, M.; Zhao, J. C.-G., Advances in Asymmetric Diastereodivergent Catalysis. *Adv. Synth. Catal.* 2017, 359, 534-575; (c) Krautwald, S.; Carreira, E. M., Stereodivergence in Asymmetric Catalysis. *J. Am. Chem. Soc.* 2017, 139, 5627-5639; (d) Beletskaya, I. P.; Nájera, C.; Yus, M., Stereodivergent Catalysis. *Chem. Rev.* 2018, 118, 5080-5200.

Examples of stereodivergent reactions of racemic starting materials: (a) Reynolds, N. T.; Rovis, T., The effect of pre-existing stereocenters in the intramolecular asymmetric Stetter reaction. Tetrahedron 2005, 61, 6368-6378; (b) Samanta, S.; Perera, S.; Zhao, C.-G., Organocatalytic Enantioselective Synthesis of Both Diastereomers of α-Hydroxyphosphinates. J. Org. Chem. 2010, 75, 1101-1106; (c) Sternativo, S.; Calandriello, A.; Costantino, F.; Testaferri, L.; Tiecco, M.; Marini, F., A Highly Enantioselective One-Pot Synthesis of Spirolactones by an Organocatalyzed Michael Addition/Cyclization Sequence. Angew. Chem. Int. Ed. 2011, 50, 9382-9385; (d) Johnston, R. C.; Cohen, D. T.; Eichman, C. C.; Scheidt, K. A.; Ha-Yeon Cheong, P., Catalytic kinetic resolution of a dynamic racemate: highly stereoselective β-lactone formation by N-heterocyclic carbene catalysis. Chem. Sci. 2014, 5, 1974-1982; (e) Romanov-Michailidis, F.; Pupier, M.; Guénée, L.; Alexakis, A., Enantioselective halogenative semi-pinacol rearrangement: a stereodivergent reaction on a racemic mixture. Chem. Commun. 2014, 50, 13461-13464; (f) Wen, G.; Su, Y.; Zhang, G.; Lin, Q.; Zhu, Y.; Zhang, Q.; Fang, X., Stereodivergent Synthesis of Chromanones and Flavanones via Intramolecular

Benzoin Reaction. Org. Lett. 2016, 18, 3980-3983; (g) Abbasov, M. E.; Hudson, B. M.; Tantillo, D. J.; Romo, D., Stereodivergent, Diels-Alderinitiated organocascades employing α,β-unsaturated acylammonium salts: scope, mechanism, and application. Chem. Sci. 2017, 8, 1511-1524; (h) Vasamsetty, L.; Kong, X.; Meng, M.; Yang, S.; Xu, W.; Reddy, P. S.; Fang, X., Divergent Dynamic Kinetic Resolution of a Racemic Mixture of Four Stereoisomers via N-Heterocyclic Carbene Organocatalysis. Chem. Asian J. 2018, 13, 3838-3844; (i) Zhao, Z.; Yang, S.; Lan, S.; Liu, I.; Liu, S.; Fang, X., Asymmetric Synthesis of Dihydronaphthalene-1,4-Diones via Carbene-Catalyzed Stereodivergent Reaction. Adv. Synth. Catal. 2019, 361, 3943-3949; (j) De Jesús Cruz, P.; Crawford, E. T.; Liu, S.; Johnson, J. S., Stereodivergent Nucleophilic Additions to Racemic Acid Derivatives: Fast Addition Outcompetes Stereoconvergence in the Archetypal Configurationally Unstable Electrophile. J. Am. Chem. Soc. 2021, 143, 16264-16273.

- (20) Bandgar, B. P.; Patil, A. V., Fluoroboric acid adsorbed on silica gel catalyzed regioselective ring opening of epoxides with nitrogen heterocycles. *Tetrahedron Lett.* 2007, 48, 173-176.
- (21) Lin, Y.; Hirschi, W. J.; Kunadia, A.; Paul, A.; Ghiviriga, I.; Abboud, K. A.; Karugu, R. W.; Vetticatt, M. J.; Hirschi, J. S.; Seidel, D., A Selenourea-Thiourea Brønsted Acid Catalyst Facilitates Asymmetric Conjugate Additions of Amines to α,β-Unsaturated Esters. *J. Am. Chem. Soc.* **2020**, *142*, 5627-5635.
- (22) See The Supporting Information for detailed descriptions of these calculations.
- (23) Bickelhaupt, F. M.; Houk, K. N., Analyzing Reaction Rates with the Distortion/Interaction-Activation Strain Model. *Angew. Chem. Int. Ed.* **2017**, *56*, 10070-10086.
- (24) Chandra Mallojjala, S.; Sarkar, R.; Karugu, R. W.; Manna, M. S.; Ray, S.; Mukherjee, S.; Hirschi, J. S., Mechanism and Origin of Remote Stereocontrol in the Organocatalytic Enantioselective Formal C(sp2)–H Alkylation Using Nitroalkanes as Alkylating Agents. *J. Am. Chem. Soc.* 2022, 144, 17399-17406.
- (25) Ess, D. H.; Houk, K. N., Distortion/Interaction Energy Control of 1,3-Dipolar Cycloaddition Reactivity. *J. Am. Chem. Soc.* **2007**, *1*29, 10646-10647.
- (26) Maji, R.; Mallojjala, S. C.; Wheeler, S. E., Chiral phosphoric acid catalysis: from numbers to insights. *Chem. Soc. Rev.* 2018, 47, 1142-1158.
- (27) Maji, R.; Wheeler, S. E., Importance of Electrostatic Effects in the Stereoselectivity of NHC-Catalyzed Kinetic Resolutions. *J. Am. Chem. Soc.* **2017**, *139*, 12441-12449.
- (28) Seguin, T. J.; Wheeler, S. E., Stacking and Electrostatic Interactions Drive the Stereoselectivity of Silylium-Ion Asymmetric Counteranion-Directed Catalysis. *Angew. Chem. Int. Ed.* **2016**, 55, 15889-15893.
- (29) Grimme, S.; Antony, J.; Ehrlich, S.; Krieg, H., A consistent and accurate ab initio parametrization of density functional dispersion correction (DFT-D) for the 94 elements H-Pu. J. Chem. Phys. 2010, 132, 154104.
- (30) Grimme, S.; Ehrlich, S.; Goerigk, L., Effect of the damping function in dispersion corrected density functional theory. *J. Comput. Chem.* **2011**, 32, 1456-1465.
- (31) Lu, T.; Chen, Q., Independent gradient model based on Hirshfeld partition: A new method for visual study of interactions in chemical systems. *J. Comput. Chem.* **2022**, *43*, 539-555.

### Table of Contents artwork

